Influence of the Protein Binding Site on the Excited States of Bacteriochlorophyll: DFT Calculations of B800 in LH2

Zhi He, Villy Sundström, and Tõnu Pullerits*

Department of Chemical Physics, Lund University, P.O. Box 124, S-22100 Lund, Sweden

Received: January 11, 2002; In Final Form: June 26, 2002

Effects of hydrogen bonding and the axial ligand interaction on the B800 band in two LH2 complexes *Rhodopseudomonas* (*Rps.*) *acidophila* and *Rhodospirillum* (*Rs.*) *molischianum* have been theoretically investigated by using density functional theory. The local electrostatic environment of the B800 bacteriochlorophyll is simulated as an atomic charge field consisting of the pigments in the protomer unit. Despite the fact that the B800 binding sites in two structures are very different, their absorption spectra are almost identical. Our calculations indicate that the charged axial ligand in *Rs. molischianum* and the hydrogen bonding in *Rps. acidophila* lead to similar red shifts, possibly explaining the above controversy. We also found (i) additional B800 bacteriochlorophyll transitions located between the Q and Soret regions for both LH2 complexes and (ii) the ligand to the B800 charge-transfer excited states in the long-wavelength region for the B800−αAsp$_6$ complex in the *Rs. molischianum* LH2 system.

I. Introduction

A photosynthetic light-harvesting (LH) antenna absorbs light energy and transfers excitation energy to a photosynthetic reaction center (RC). Photosynthetic purple bacteria contain two types of light-harvesting antennae: (i) the core antenna LH1, which surrounds the RC, and (ii) the peripheral antenna LH2, which transfers excitation energy to the RC via the LH1. All of these antenna complexes have a similar arrangement. They are constructed from a basic unit containing two polypeptides, α and β, to which the bacteriochlorophyll (BChl) *a* and carotenoid pigments are bound. For example, in LH2 complexes, one (or possibly two) carotenoid and three BChl *a* molecules are bound per $\alpha\beta$ polypeptide pair. The BChls are usually labeled according to their peak Q_y absorption wavelengths as B800 and αB850 or βB850.

A few years ago, the structures of the LH2 antennae of *Rhodopseudomonas (Rps.) acidophila*[1] and *Rhodospirillum (Rs.) molischianum*[2] became known, which generated enormous interest in the study of these complexes. Overall, both structures are very similar. They contain two rings of BChl *a* molecules. One ring comprises B850 BChls with their macrocycles perpendicular to the membrane plane. In another ring, B800, BChl molecules are nearly parallel to the membrane plane in *Rps. acidophila*, whereas they are tilted by 38° in the case of *Rs. molischianum*.[3] The carotenoid molecules span these two rings. The carotenoids of *Rps. acidophila* and *Rs. molischianum*, rhodopin glucoside and lycopene, respectively, have the same number of conjugated C=C bonds, $n = 11$. *Rps. acidophila* contains nine, and *Rs. molischianum*, eight basic units.

The spectral properties of the individual pigments within the antenna complexes are strongly dependent on the interactions with their immediate environment. It is generally accepted that two different interactions underlie the red shift of the BChl absorption in the light-harvesting pigment proteins of purple bacteria: (i) pigment−pigment exciton coupling and (ii) the tuning of the individual monomer absorption by interactions with the surrounding protein. Because of the relatively large separation between adjacent B800 molecules, excitonic effects are unimportant for the B800 ring.[4] Thus, the B800−protein interactions play a major role in affecting the excited states of the B800 BChl. In general, the protein influences the transition energies of the pigment molecules via dispersive forces due to the polarizabilities. This can be seen as a solvent shift (usually toward red). Besides this general influnce, Bchl *a* molecules in LH2 complexes have two specific interactions with protein—hydrogen bonding and axial ligation. The former has been well documented experimentally by demonstrating that the formation of hydrogen bonds between the BChl molecules and protein can modify the absorption of the BChl molecules.[5−8] Particularly, it has been observed that a certain proportion of the red shift (ca. 10 nm) of the lowest-energy transition (Q_y) of the B800 molecules is due to the hydrogen bonding of its acetyl carbonyl in *Rhodobacter sphaeroides* LH2 complex.[9] Similar hydrogen bonding occurs in B800 of *Rps. acidophila*.[10] However, no H-bond has been reported between the B800 and protein in the *Rs. molischianum* LH2 complex. Also, the axial ligands of B800 are very different in these two LH2s. In *Rps. acidophila*, the central magnesium of B800 is ligated by a formyl methionine, αfMet$_1$, whereas in *Rs. molischianum*, it is ligated by a charged residue aspartate (αAsp$_6$). How do the different amino acids in the protein environment of the B800 pigments influence their absorption spectra? In this article, we use modern quantum chemistry methods to study the effects of the hydrogen bonding and axial ligand interactions on the absorption properties of the B800 pigments in two LH2 complexes: *Rps. acidophila* and *Rs. molischianum*.

For a review of the early computational studies of the BChl electronic structure, see ref 11. The possible origin of the spectral shifts of the pigment molecules in vivo has been addressed. Parson and Warshel[12] found that if the acetyl group of a special pair of BChl from the reaction center of *Rps. viridis* is rotated, then the position of the lowest-energy absorption band varies over a range of about 50 nm. Later studies of a so-called FMO

* Corresponding author. E-mail: Tonu.Pullerits@chemphys.lu.se. Phone: +46 46 2228131. Fax: +46 46 2224119.

10.1021/jp020063z CCC: $22.00
Published on Web 10/10/2002

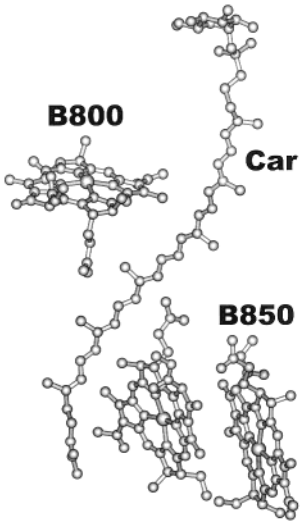

Figure 1. Organization of pigments in the protomer unit of the *Rps. acidophila* complex. Note that for simplicity the phytyl chain of the BChl has been removed in the Figure but included in all calculations.

antenna complex from *Prosthecochloris (P.) aestuarii* suggest that the rotation of the acetyl group out from the coplanar orientation with the porphyrin ring would lead to a blue shift of the Q_y transition,[13] whereas usually in vivo spectra are red-shifted. Furthermore, assignment of the Q_y transition energies of the BChls in FMO from *P. aestuarii*[14] strongly suggests that BChl number 3 (for the numbering, see ref 15) has the lowest transition energy. The same molecule is given the highest transition energy according to the calculations based on the acetyl group rotation.[13] There does not seem to be any obvious correlation between the BChl Q_y transition energy and the acetyl group orientation. Consequently, the spectral shifts induced by the H-bonding of the acetyl carbonyl are not likely due to the possible change of the acetyl group orientation alone. Quite a number of LH2 studies that apply quantum chemistry methods have been published recently.[16−19] These articles are mainly concerned with exciton couplings in the strongly coupled B850 ring.

The following section briefly describes our computational strategy. Effects of protein environments on the B800 band are discussed in section III, where we distinguish between direct and indirect effects. Comparison of the B800 BChl structures and their calculated excitation energies in the local LH2 electrostatic environments reveals the indirect effect that is induced by the distortion of the B800 structure due to their different local environments. The direct effects usually involve the participation of hydrogen bonds and axial ligation interactions. In our calculations, we permit the B800 BChl to be hydrogen bonded to βArg_{20} or to be ligated by $\alpha fMet_1$ (or αAsp_6) to examine the direct effects of hydrogen bonding and axial ligation on the B800 excited states. The conclusions are finally drawn in section IV.

II. Computational Methods

The basic unit of the LH2 antenna complexes (a so-called protomer unit) contains the following pigment molecules: a single B800, a pair of B850s, and a carotenoid (rhodopin glucoside in *Rps. acidophila*, lycopene in *Rs. molischianum*). Figure 1 displays the structure of these pigments in the protomer unit of the *Rps. acidophila* complex.[1] The nine (or eight) protomer units constitute a complete structure of the pigments in LH2. The protomer unit is the starting point of our calculations. The local electrostatic environment of the B800 due to nearby pigments is represented via a charge field involving two B850 BChls and one carotenoid. In such a charge field, the effects of some related amino acids on the excited states of B800 will be examined using time-dependent density functional theory (TDDFT) with the three-parameter Lee−Yang−Parr (B3LYP) functional.[20] Our calculations are based on the crystal structures of *Rps. acidophila*[1] and *Rs. molischianum*[2] and are carried out by the Gaussian 98 program.[21]

Because the current resolution of the LH2 structure is not sufficient to resolve hydrogen atoms, the missing hydrogen positions in B800, α,βB850, Car, and the amino acid residues (i.e., Arg, Met) are generated by using individual geometry optimizations while keeping the other atoms fixed. The optimizations are performed at the restricted Hartree−Fock (RHF) level with the 6-31G basis set. To build up the electric field of the environment, atomic point charges of the BChls and Car are obtained from the RHF/6-31G calculation for the four-pigment supermolecular complex shown in Figure 1 by using the Mulliken population analysis, as described in our previous work.[22] This electrostatic field of nearby pigments was used in all of our TDDFT calculations. We have calculated the first 10 excited states of B800. Recent TDDFT calculations of the ionization potentials and electron affinities of BChl and bacteriopheophytin have suggested a need to use a rather extensive basis set for obtaining convergent results.[23] The split-valence basis sets augmented with polarization functions on the C, N, O, and Mg atoms (SVP) have been employed in the TDDFT study of chlorophyll *a* electronic transitions by Sundholm.[24] Therefore, the SVP basis set is also used in most of our TDDFT calculations. We have compared the SVP basis set calculations with smaller, computationally faster 6-31G basis set calculations and did not find big differences. Consequently, the 6-31G basis set is applied in some of our calculations, greatly reducing our computational effort.

The B800 BChl binding site in LH2 of *Rps. acidophila* is characterized by two important features that affect its electronic spectra: (i) hydrogen bonding with βArg_{20} and (ii) axial ligand interaction between B800 and the amino acid residue $\alpha fMet_1$.[1] To consider the hydrogen bonding and axial ligand interaction, we employ a second optimization step to refine the hydrogen atom positions in the two amino acids arginine and formyl methionine after initial geometry optimizations of the hydrogen atoms for each individual molecule. The hydrogen positions of the possible hydrogen-bond region and near the Mg atom in the βArg_{20} and $\alpha fMet_1$ amino acids are reoptimized at the RHF/6-31G level for the B800−βArg $_{20}$−$\alpha fMet_1$ complex illustrated in Figure 3.

In LH2 of *Rs. molischianum*, it is known that the B800 BChl is ligated to αAsp_6 (rather than to a formyl methionine as in *Rps. acidophila*), which normally has a negative charge. We have analyzed the crystal structure of *Rs. molischianum* in detail and have confirmed that no strong hydrogen bond is formed between B800 and nearby amino acids. Despite the fact that the protein binding sites for the B800 BChl in the LH2 of *Rps. acidophila* and *Rs. molischianum* are so different, the B800 BChls in these two complexes have almost identical B800 absorption spectra. It stimulates us to take a closer look at their low-lying excited states in LH2. In particular, how are these states affected by specific factors from the protein environment: hydrogen bonding, axial ligation, and nearby charged amino acids?

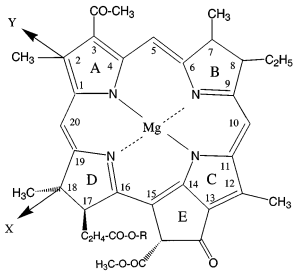

Figure 2. Molecular structure of the B800 BChl and definition of the molecular axes, where R = phytyl.

III. Results and Discussion

Protein environments of BChl pigments influence their absorption spectra, sometimes substantially. In the present work, we investigate the effects of the protein binding sites (the hydrogen bonding and axial ligation) on the B800 excitation energies, predicted by the TDDFT calculations. These effects can be divided into the direct influence induced by changes in the electronic structure of B800 due to the interactions with nearby amino acids and the indirect influence via "fixing" the BChl in a different structure due to the difference in the hydrogen bonding pattern or the different axial ligand interactions. To better understand the origin of the spectral changes, we first compare the two B800 structures and calculate their excited states in the local electrostatic field of the nearby pigment molecules. We continue by extending the system via including the hydrogen bonding amino acids and axial ligand in the calculations.

Comparison of the B800 BChl Structure in Two LH2 Complexes. The most important geometry parameter for the B800 structure is bond lengths in the cyclic π system (see Figure 2). This is the primary factor that controls the electronic properties of the B800 BChl. Table 1 compares the distances between atoms in the porphyrin ring for the LH2 of *Rps. acidophila* and *Rs. molischianum*. We point out that the X-ray diffraction resolution of these structures are quite similar (2.5 Å for *Rps. acidophila* and 2.4 Å for *Rs. molischianum*), justifying such a comparison. However, the experimental errors of individual atomic coordinates may be larger than the differences we report here.

In the two structures, the magnesium atom is almost at the center of the planar porphyrin ring. However, from the distance between the Mg atom and three-nitrogen (NA−NB−NC) plane, one finds that the magnesium atom in the *Rps. acidophila* structure is slightly out of the plane of the porphyrin ring, which indicates the different interactions between B800 and its ligand in the two LH2 systems. At first glance, the largest difference in the bond lengths of the cyclic π system of the two structures is the bond length between the C_{13} and C_{14} atoms in the C ring. For the *Rps. acidophila* structur,e it is about 0.07 Å shorter than the corresponding bond length in *Rs. molischianum* (1.439 Å), whereas the calculated distance $C_{13}-C_{14}$ in BChl *a*, the monomer structure fully optimized at the semiempirical PM3 level, is even longer, 1.475 Å.[25] Another significant difference in the two B800 structures is in the B ring, where all three C−C bonds, namely C_6-C_7, C_7-C_8, and C_8-C_9 bonds, are single bonds, which should be longer than 1.5 Å. Unexpectedly, the C_8-C_9 bond length in the *Rps. acidophila* complex is rather short, only 1.474 Å. This means that the C_8-C_9 bond, at least in part, can participate in the conjugated π system. The longest bond length in the cyclic π system for the *Rps. acidophila* complex is the 1.494-Å C_3-C_4 bond. This bond is very close to the hydrogen bond between the acetyl carbonyl oxygen from ring A and the βArg$_{20}$ amino acid. Consequently, this bond lengthening can be the result of the hydrogen bonding.

TABLE 1: Comparison of Heavy Atom Distances (Å) in X-ray Crystal Structures of B800 Bchl in LH2 Complexes along with Calculated Molecular Structures of BChl *a* and Chl *a* in Vacuum

	B800 BChl in LH2 complexes			
distances[a]	*Rps. acidophila*	*Rs. molischianum*	BChl *a*[b]	Chl *a*[c]
1−2	1.444	1.443	1.423	1.456
2−3	1.352	1.361	1.407	1.400
3−4	1.494	1.441	1.438	1.457
4−5	1.374	1.391	1.432	1.406
5−6	1.358	1.383	1.354	1.417
6−7	1.505	1.503	1.517	1.461
7−8	1.503	1.514	1.548	1.390
8−9	1.474	1.506	1.517	1.463
9−10	1.338	1.391	1.446	1.414
10−11	1.331	1.383	1.355	1.410
11−12	1.469	1.458	1.495	1.462
12−13	1.377	1.362	1.363	1.402
13−14	1.368	1.439	1.475	1.430
14−15	1.358	1.371	1.388	1.419
15−16	1.419	1.384	1.402	1.395
16−17	1.503	1.508	1.527	1.526
17−18	1.510	1.514	1.557	1.555
18−19	1.512	1.525	1.516	1.532
19−20	1.342	1.403	1.356	1.400
20−1	1.350	1.400	1.430	1.421
NA-1	1.398	1.373	1.400	1.373
NA-4	1.396	1.374	1.380	1.381
NB-6	1.415	1.404	1.438	1.373
NB-9	1.400	1.407	1.336	1.382
NC-11	1.400	1.373	1.445	1.396
NC-14	1.347	1.359	1.353	1.343
ND-16	1.422	1.394	1.346	1.379
ND-19	1.409	1.392	1.431	1.365
Mg−NA	2.042	2.051	2.325	2.046
Mg−NB	2.023	2.066	2.467	2.082
Mg−NC	1.998	1.993	1.830	2.031
Mg−ND	2.070	2.133	1.829	2.165
A, B, C, Mg	0.264	0.073	0.096	0.026
NA−NB	2.891	2.931	3.052	2.960
NA−NC	4.006	4.041	4.067	4.077
NA−ND	2.880	2.979	2.928	3.013
NB−NC	2.762	2.808	2.732	2.841
NB−ND	4.060	4.198	4.268	4.245
NC−ND	2.875	2.942	3.074	2.960

[a] The number 1 (or 2, ...) refers to the C1 (or C2, ...) atom, whereas NA is nitrogen in ring A, as shown in Figure 2. The notation A, B, C, Mg denotes the distance between plane NA−NB−NC and the Mg atom (see Figure 2). [b] The calculated structure was fully optimized at the semiempirical PM3.[21] [c] The complete structure was optimized at the resolution of the identity density functional theory (RI-DFT) level.[29]

In addition, the difference between conjugated single- and double-bond lengths in *Rps. acidophila* is larger than that in *Rs. molischianum*. The shortest and longest bond lengths in the cyclic π system for the *Rs. molischianum* structure are 1.361 Å (the C_2-C_3 bond) and 1.458 Å (the $C_{11}-C_{12}$ bond). The difference between them (0.097 Å) is smaller than the corresponding difference (0.163 Å) in the *Rps. acidophila* structure. The C−C bonds out of rings A and C (e.g., $C_{20}-C_1$,C_4-C_5,-IC_5-C_6,C_9-C_{10},...) in the *Rps. acidophila* structure are shorter than those in the *Rs. molischianum* structure, except for the $C_{15}-C_{16}$ bond. Most of the C−N bond lengths in the former are, however, longer than the corresponding bond lengths in the latter. Overall, the single (double) bonds in the cyclic π system of *Rs. molischianum* become shorter (longer) than those of *Rps. acidophila*. This indicates that the conjugated π electrons of the B800 BChl in the *Rs. molischianum* structure are more delocalized than in the *Rps. acidophila* structure. From this point

TABLE 2: Singlet Excitation Wavelengths (nm) and Oscillator Strengths (in Parentheses) for B800 BChl in the Charge Field of Neighboring Pigment Molecules as Calculated with TDDFT/B3LYP and DFT-MRCI Methods[a]

	B800 BChl in LH2 complexes				
	B3LYP/6-31G	B3LYP/SVP	B3LYP/6-31G	B3LYP/SVP	BChl *a*
	Rps. acidophila		*Rs. molischianum*		
2A	653 (0.0188)	670 (0.3632)	681 (0.0175)	693 (0.3567)	Q_y 771
3A	523 (0.0042)	534 (0.0425)	553 (0.0051)	561 (0.0565)	Q_x 573
4A	426 (0.0000)	437 (0.0002)	499 (0.0000)	506 (0.0001)	
5A	423 (0.0000)	420 (0.0002)	429 (0.0034)	431 (0.0543)	
6A	408 (0.0000)	411 (0.0001)	403 (0.0022)	409 (0.0004)	
7A	395 (0.0005)	400 (0.0043)	399 (0.0071)	403 (0.0433)	
8A	373 (0.0179)	380 (0.1644)	389 (0.0080)	389 (0.1653)	B_x 390
9A	369 (0.0002)	369 (0.0822)	378 (0.0003)	377 (0.0001)	
10A	360 (0.0288)	363 (0.2646)	378 (0.0003)	368 (0.1582)	
11A	335 (0.0366)	345 (0.0202)	367 (0.0173)	365 (0.0164)	B_y 357

[a] Data for the B transitions are underlined. Experimental results for BChl *a* in diethyl ether are from ref 32.

TABLE 3: Hydrogen-Bond Geometry Parameters for the B800−βArg$_{20}$ Complex[a]

$d_{O...H}$ (Å)		∠*H*...O...N (deg)	
O...H_1	2.306	∠H_1ON_1	25.6
O...H_2	1.989	∠H_2ON_2	18.3
criterion:[b]			
O...H	<2.4	∠*HON* (or O)	<35

[a] Atom labels are defined in Figure 3. [b] See ref 26.

of view, the low-lying excitation energies of the B800 BChl in the former could be lower than those in the latter. Furthermore, the rather short C_8-C_9 bond in *Rps. acidophila* probably lengthens the π-electron pathway, also leading to lower excited states of the B800 BChl. In the following discussion, we will see that the effect of the bond shortening does not dominate the excitation energies of the single B800 molecule.

Excited States of B800 in the Local LH2 Electrostatic Field of Other Pigments. Most quantum chemical methods fail to give accurate energies for large systems. Sometimes the energies are systematically scaled to make comparison with experiment easier.[26] Because in the current work we mainly compare the calculations of two systems, we have chosen not to perform any scaling.

Table 2 summarizes the TDDFT/B3LYP energies and oscillator strengths for the B800 BChl in charge fields of the nearby pigments in *Rps. acidophila* and *Rs. molischianum* along with the experimental transition energies. The B3LYP calculations with the two basis sets (6-31G and SVP) yield the first two lowest excited states (denoted as 2A, 3A in Table 2 and assigned to Q_y, Q_x; 1A refers to the ground state) of the B800 BChl in the *Rps. acidophila* complex as 0.06−0.13 eV higher than those in the *Rs. molischianum* complex. In other words, the red shifts of around 23 and 27 nm for Q_y and Q_x, respectively, are calculated as a result of the more-delocalized conjugated π electrons of the B800 BChl in the *Rs. molischianum* structure. But no difference of the Q_y and Q_x absorptions in these two LH2 complexes has been observed in experiment. The higher lying Soret (B) states, marked with underlines in Table 2, are located at 367−389 nm for both of the two LH2 complexes. Between the Q and B states, we found four (or seven) transitions. Except a weak transition obtained at 400 nm in the B3LYP/SVP calculation, all of these transitions are optically forbidden in *Rps. acidophila* for they carry almost zero oscillator strengths (<0.0010), presented as italics in Table 3. In contrast, two (or four) allowed transitions of the B800 BChl in *Rs. molischianum* are obtained at about 400−430 nm with the SVP (or 6-31G) basis set (see Table 2). As the 6-31G basis set is extended to the SVP basis set, all transition energies are decreased.

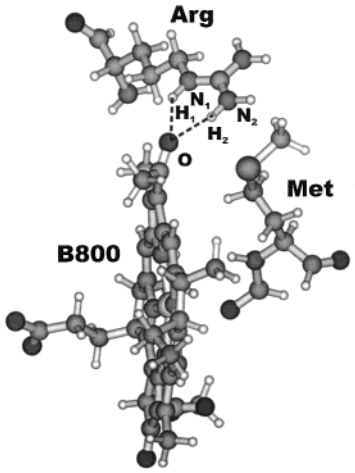

Figure 3. Molecular complex used for studying the effects of the hydrogen bonding and the axial ligation on the B800 excitation energies. The dashed lines indicate the intermolecular hydrogen bonds.

It is worthwhile to mention that the SVP basis set clearly produces lower excitation energies and leads to larger oscillator strengths for the main transitions. However, we found that the SVP basis set does not offer a significant improvement over the 6-31G basis set for studying the effects of hydrogen bonding and axial ligand interaction on the Q_y and Q_x transitions because both basis sets provide rather similar band shifts, as we will see below. Therefore, the 6-31G basis set is applied in some of the calculations, whereas the SVP basis set is used in the final calculation to examine the effects of hydrogen bonds and ligand interaction. For clarity, B transitions are always marked with underlines, and transitions with very small oscillator strengths (<0.0010) are in italics in the tables.

Hydrogen Bonding. It is known from early mutagenesis work that the βArg$_{20}$ residue forms part of the binding site for the B800 BChl in the purple bacteria.[27,28] Both the X-ray structure[1] and Raman spectroscopy[29] revealed a strong hydrogen bond between the acetyl carbonyl group of B800 and the βArg$_{20}$ residue. To obtain more information about this B800 binding site, let us look at the structure of the B800−βArg$_{20}$−αfMet$_1$ complex of *Rps. acidophila* in Figure 3. We can identify two intermolecular hydrogen bonds between the B800 BChl and the βArg$_{20}$ residue (see Figure 3) by applying the criteria of the intermolecular hydrogen bonds: (i) a hydrogen-acceptor distance that is shorter than 2.4 Å and (ii) the angle between the hydrogen, the atom to which the hydrogen is covalently bound, and the acceptor should be smaller than 35°.[30]

Table 3 presents the relevant hydrogen-bond structural parameters. Although the N_2 atom (for notation, see Figure 3) may be involved in an Asp-Arg salt bridge that is not included in the present study, the shorter hydrogen-acceptor distance $d_{O\cdots H_2}$ (1.989 Å) and the smaller angle ∠H_2ON_2 (18.3°) suggest that the H-bond N_2-H_2...O is stronger than the other H-bond N_1-H_1...O. This is confirmed by comparing the charge distributions of the B800−βArg$_{20}$−αfMet$_1$ complex and the separate B800 BChl and βArg$_{20}$ amino acid. The largest difference in the charges appears on the acetyl carbonyl oxygen of the B800 BChl. Its atomic charge (−0.6905) in the complex is much more negative than that (−0.5393) of the individual molecule. Correspondingly, the charge of the H_2 atom (0.5150) in the complex is much more positive than the charge (0.4288) in the individual βArg$_{20}$ amino acid, the difference of which is larger

than that of the charges computed for the H_1 atom. As we have seen above, the strong H-bonds directly affect the structure of the B800 BChl, lengthening the nearby conjugated C−C bond. This change could indirectly influence the excitation energies of the B800 BChl.

To clarify whether the hydrogen bonding directly influences the B800 excited states, we performed the B3LYP/6-31G calculations of the B800−βArg$_{20}$ complex with the same charge field of nearby pigment molecules as before. The results are summarized in Table 5. Comparing these results with B800-only calculations, we conclude that the presence of hydrogen bonding induces an ∼18-nm red shift of the Q_y and Q_x transitions. This theoretical estimate of the H-bond effect on the Q_y energy is in good agreement with the experimental findings in the *Rhodobacter sphaeroides* LH2 complex.[9,31] We also found that the direction of the transition dipole moment for the Q_y state is almost unchanged by the hydrogen bonds; it remains almost parallel to the *Y* axis of the B800 BChl defined as the N(C)−N(A) direction (see Figure 2), whereas the orientations of the Q_x is somewhat changed. This result can, in principle, be verified by optical experiments with polarized light. The higher-energy transitions are quite significantly changed by the hydrogen bonding. Most remarkably, a new weak transition (oscillator strength of 0.0024) appears between the Q and B bands. Additional electronic transitions, which are not included in the conventional Gouterman model of the Chl electronic structure,[32] have been reported in earlier TDDFT studies of Chl *a*[24,33] and BChl in LH2.[34] No clear experimental assignment of additional transitions has been made so far. This may be due to their weak transition dipoles. It has been also suggested that these transitions are artifacts of calculations.[33] However, the visible absorption spectrum of Chl and BChl has an obvious nonzero background absorption outside the main Q and B bands. This background is usually argued to have a vibrational origin. Here we point out a recent study of B800 to B850 excitation transfer where the B800 BChl was changed to other similar molecules with shifted absorption spectra.[35] Förter spectral overlap calculations where the region of vibrational transitions was also included could not explain the change in the transfer rates for the most blue-shifted systems. The controversy can be solved by additional weak electronic transitions, very similar to the ones we have reported here.

Axial Ligation. In the same way, we study another part of the protein binding site, the axial ligand. In the *Rps. acidophila* complex, we perform calculations for a B800−αfMet$_1$ complex in the charge field of the nearby pigments (see Table 4). In this case, the B800 BChl is linked to a formyl oxygen of the αfMet$_1$. We found a red shift (∼10 nm) of the Q_x transition and no significant effect on the Q_y and B transitions (underlined in Table 4). We can conclude that in *Rps. acidophila* the axial ligand αfMet$_1$ does not influence the B800 Q_y transition as strongly as the charged hydrogen bonding residue βArg$_{20}$. As we will see, a charged ligand can produce large effects.

The Mg ligand of the B800 BChl in *Rs. molischianum*, αAsp$_6$, has a negative charge. The TDDFT calculations of the B800−αAsp$_6$ complex lead to large red shifts of the B800 Q_y and Q_x transitions. Interestingly, the B3LYP/SVP calculations predict eight lower intermolecular charge-transfer (CT) excited states of the B800−αAsp$_6$ complex involving the valence occupied orbitals (αAsp $_6$) → p* (B800) excitations (see Table 5). Three CT transitions marked in boldface in Table 6 are distributed over the region of Q bands. The lowest CT state (940.3 nm) is below the Q_y transition. A CT state with a relatively strong transition dipole moment lies between Q_y and Q_x. Another CT state is slightly higher than the Q_x transition. The B3LYP/6-31G calculations provide very similar CT states but with smaller oscillator strengths.

Experiments with (metal-substituted) BChls have shown that the Q_x transition energy is more sensitive to the axial ligation than the Q_y energy.[36] The behavior was qualitatively explained by substantial involvment of the nitrogen and the central metal atoms in the orbitals that contribute to the main configuration of the Q_x transition. Our DFT calculations are in good agreement with this trend. Furthermore, we obtained a small blue shift of

TABLE 4: Comparison of Wavelengths λ (nm) and Oscillator Strengths *f* for B800 BChl Alone and for Its Complexes (B800−βArg$_{20}$ and B800−αfMet$_1$) as Computed with the B3LYP/6-31G Calculations[a]

	B800			B800−βArg$_{20}$			B800−αfMet$_1$	
states	λ	*f*		λ	*f*		λ	*f*
2*A*	653.3	0.0188		671.4	0.0210		652.1	0.0186
			Q_y	(18.1)			(−1.2)	
3*A*	522.4	0.0042		555.9	0.0000		533.3	0.0042
						Q_x	(10.9)	
4*A*	425.5	0.0000		540.3	0.0052		462.0	0.0002
			Q_x	(17.9)				
5*A*	423.8	0.0000		446.9	0.0000		431.4	0.0000
6*A*	408.3	0.0000		443.5	0.0024		425.5	0.0000
7*A*	395.3	0.0005		408.5	0.0000		415.5	0.0000
8*A*	373.4	0.0179		403.4	0.0002		404.8	0.0001
9*A*	369.0	0.0002		379.5	0.0182		402.8	0.0001
10*A*	360.1	0.0288		376.6	0.0000		397.5	0.0003
11*A*	335.1	0.0366		373.2	0.0014		377.0	0.0170

[a] All calculations are performed in the same charge field that describes the local electrostatic LH2 (*Rps. acidophila*) environment because of the nearby pigments. The values in parentheses denote the wavelength shifts. Transitions with a negligible oscillator strength are in italics.

TABLE 5: Comparison of Calculated Excitation Energies *E* (eV), Wavelengths λ (nm), and Oscillator Strengths *f* for B800 BChl and Its Complex B800−Asp in *Rs. molischiamum*[a]

states	B800				B800−Asp		
6-31G	*E*	λ	*f*		*E*	λ	*f*
				CT[b]	*0.65*	*1909.1*	*0.0000*
				CT	*1.20*	*1032.0*	*0.0000*
				CT	*1.37*	*905.1*	*0.0003*
				CT	*1.69*	*732.9*	*0.0000*
Q_y	1.82	680.0	0.0175		1.79	692.2	0.0163
						(12.2)	
				CT	*1.96*	*631.8*	*0.0007*
Q_x	2.24	554.0	0.0051		2.06	601.9	0.0046
						(47.9)	
				CT	*2.18*	*567.8*	*0.0002*
				CT	**2.20**	**563.4**	**0.0014**
				CT	*2.25*	*550.4*	*0.0000*
SVP							
				CT	*0.53*	*2351.8*	*0.0008*
				CT	*1.15*	*1078.6*	*0.0001*
				CT	**1.32**	**940.3**	**0.0048**
Q_y	1.79	694.0	0.3567		1.75	707.2	0.3299
						(13.2)	
				CT	*1.80*	*688.4*	*0.0002*
				CT	**1.88**	**660.8**	**0.0166**
Q_x	2.21	561.5	0.0565		2.05	604.0	0.0551
						(42.5)	
				CT	**2.10**	**590.2**	**0.0100**
				CT	*2.22*	*558.2*	*0.0003*
				CT	*2.25*	*550.4*	*0.0001*

[a] All calculations are carried out in the charge field consisting of α,βB850 BChls and lycopene. The values in parentheses denote the wavelength shifts. [b] The ligand-to-B800 charge-transfer states.

TABLE 6: Comparison of Excitation Energies *E* (eV), Wavelengths λ (nm), and Oscillator Strengths *f* for B800 BChl Alone and for Its Complex B800−βArg$_{20}$−αfMet$_1$ as Computed with the B3LYP DFT Method[a]

states	B800			P^c		B800−βArg$_{20}$−αfMet$_1$			
6-31G[b]	*E*	λ	*f*	(deg)		*E*	λ	*f*	*P* (deg)
2*A* (Q_y)	1.90	653.3	0.0188	2.5		1.85	671.0 (17.7)	0.4083	3.2
3*A* (Q_x)	2.37	522.4	0.0042	93.2		2.25	551.4 (29.0)	0.0642	100.7
4*A*	3.32	373.4	0.0179	94.4		2.82	439.9	0.0185	131.1
5*A*	3.44	360.1	0.0288	87.3	(CT)	2.83	438.4	0.0059	66.5
6*A*	3.70	335.1	0.0366	140.3		3.07	403.7	0.0018	100.2
7*A*						3.25	381.3	0.1515	49.4
SVP									
2*A* (Q_y)	1.85	668.8	0.3632	3.1		1.81	685.5 (16.7)	0.4039	3.6
3*A* (Q_x)	2.32	533.8	0.0425	88.8		2.23	555.8 (22.0)	0.0548	97.5
4*A*	*2.84*	*435.9*	*0.0002*	*60.7*		*2.31*	*537.8*	*0.0000*	*81.8*
5*A*	*2.95*	*420.9*	*0.0002*	*61.5*		*2.72*	*455.0*	*0.0002*	*127.5*
6*A*	*3.02*	*409.9*	*0.0001*	*92.2*	(CT)	*2.79*	*443.8*	*0.0006*	*27.8*
7*A*	3.10	400.5	0.0043	100.5		2.84	436.5	0.0348	51.1
8*A*	3.26	380.3	0.1644	94.6		3.04	408.3	0.0011	108.6
9*A*	3.36	369.5	0.0822	88.5		*3.06*	*405.1*	*0.0000*	*136.8*
10*A*	3.42	362.7	0.2646	87.6		3.24	382.1	0.1509	65.2
11*A*	3.59	345.1	0.0202	63.8		*3.29*	*376.8*	*0.0008*	*52.3*

[a] All calculations are performed in the charge field. The values in parentheses denote the wavelength shifts. [b] Only transitions with nonzero oscillator strengths ($\geq$0.0010) are presented. [c] Polarization values, which refer to the angles of the transition dipole moments with respect to the *Y* axis of B800 BChl defined as the N(C)−N(A) (or N(A)−N(C)) direction displayed in Figure 2, are given in degrees.

Q_y upon ligation of the B800 with αfMet$_1$. Remarkably, in Ni-substituted BChl, the blue shift of the Q_y band due to the ligation was observed.[37]

In summary, we have found significant red shifts of the B800 Q_y band induced by nearby amino acids in both *Rps. acidophila* and *Rs. molischianum*. However, the source of the red shift is different. In *Rps. acidophila*, the shift originates mainly from the hydrogen-bonding positively charged residue βArg$_{20}$, whereas in *Rs. molischianum*, the negatively charged axial ligand αAsp$_6$ is the source of the shift. The neutral axial ligand αfMet$_1$ in *Rps. acidophila* does not lead to any significant change. B850 CIS calculations have also found red shifts due to the positively charged His ligand.[16]

Effects of the Hydrogen Bonding and the Axial Ligand in *Rps. acidophila*. Up to this point, we have studied the effects due to the hydrogen bonding and axial ligands separately, and a question arises: to what extent are these effects additive? We address this issue by performing calculations with the B800−βArg$_{20}$−αfMet$_1$ complex of *Rps. acidophila*. We started with the RHF/6-31G calculation of the ground-state charge distribution of the B800−βArg$_{20}$−αfMet$_1$ complex and found that the axial ligand interaction leads to a more positive charge (1.5482 → 1.5997) for the Mg atom in the B800 BChl and, correspondingly, a more negative charge (−0.7500 → − 0.8195) for the formyl oxygen of the αfMet$_1$. An analysis of the charge distributions for the B800 and its surroundings (βArg$_{20}$ and αfMet$_1$) shows that small intermolecular charge transfer accompanies the hydrogen bonding and the axial ligand interaction, as the total partial charges computed for each unit of the B800−βArg$_{20}$−αfMet$_1$ complex are −0.0016 (B800), 0.9494 (βArg$_{20}$), and 0.0522 (αfMet$_1$). In other words, approximately 0.0015−0.0522 electrons are transferred between the two amino acids and the B800 BChl. This implies that the hydrogen bonding and the axial ligand interaction might be concerted. In Table 6, we compare the excitation energies of the individual B800 BChl and its complex B800−βArg$_{20}$−αfMet$_1$ calculated with two basis sets (6-31G and SVP). We can see that the effects on the Q_y and Q_x transitions are almost equal to the sum of the individual effects of hydrogen bonding and axial ligation in the B3LYP/6-31G calculations. The large red shift (29.0 nm) of the Q_x band has an ∼40% contribution from the axial ligand interaction and an ∼60% contribution from the hydrogen bonding. The hydrogen bonding induces the entire calculated red shift (17.7 nm) of the Q_y transition. It seems that both effects are almost independent of each other. However, we also found that the hydrogen bonding in combination with the axial ligand interaction (i) greatly increases the oscillator strength of the Q_y and Q_x and (ii) makes one of the two originally forbidden transitions between the Q and B bands become somewhat allowed (439.9 nm). The other transition (403.7 nm) remains rather weak. Between these two transitions appears a CT state (438.4 nm) involving the valence π (fMet$_1$) → p* (B800) excitations (439.9 nm). Extension to the SVP basis set red-shifts the CT state to 443.8 nm and decreases the oscillator strength (0.0059 → 0.0006). The two B800 transitions (436.5 and 408.3 nm) between the Q and B bands can be further confirmed in the B3LYP/SVP calculations.

IV. Conclusions

The effects of the hydrogen bonding and the axial ligand interaction on the B800 band in the two LH2 complexes have been investigated in this study. The local electrostatic environment of the B800 BChl is described by an atomic charge field consisting of the pigments in the protomer unit. In such a charge field, we have performed a series of TDDFT calculations for the B800 BChl with (or without) its nearby amino acids. Our TDDFT calculations show that the differences in the B800 structures of the two LH2 complexes (i.e., *Rps. acidophila* and *Rs. molischianum*) give rise to different Q_y transition energies (ca. 25 nm). At this stage, we cannot decide whether this difference can be fully attributed to effects due to the different LH2 environments or whether it is partially due to the limited resolution of the 3D structures of the two LH2 complexes.

To account for the direct effects of the hydrogen bonding of the amino acid and axial ligand interactions, we carried out calculations of B800−protein complexes where up to two amino acids were included. We conclude (i) that the hydrogen bonds and axial ligation exert significant influence on the Q_y and Q_x bands of the B800 BChl in *Rps. acidophila*, leading to an ∼17-nm red shift of the Q_y, which is mostly due to the hydrogen bonding, and a 22−29-nm red shift of the Q_x contributed by both hydrogen bonding and axial ligation and (ii) that in *Rs. molischianum*, where there are no known hydrogen bonds, the red shift due to the axial ligation is ∼12 nm for the Q_y and 43−48 nm for the Q_x transition. The calculations also indicated additional electronic excited states of the B800 BChl between the Q and B transition regions. A number of intermolecular CT excited states were identified for the B800−αAsp$_6$ complex in the *Rs. molischianum* LH2 system.

Acknowledgment. We thank Dr. J. L. Herek and Dr. T. Polivka for stimulating discussions. This work was supported by the Swedish Research Council. Calculations were partially carried out using facilities of the National Supercomputer Center (NSC) in Linköping, Sweden.

References and Notes

(1) McDermott, G.; Prince, S. M.; Freer, A. A.; Hawthornthwaite-Lawless, A. M.; Papiz, M. Z.; Cogdell, R. J.; Isaacs, N. W. *Nature (London)* **1995**, *374*, 517.

(2) Koepke, J.; Hu, X.; Muenke, C.; Schulten, K.; Michel, H. *Structure* **1996**, *4*, 581.
(3) Beekman, L. M. P.; Frese, R. N.; Fowler, G. J. S.; Picorel, R.; Codell, R. J.; van Stokkum, I. H. M.; Hunter, C. N.; van Grondelle, R. *J. Phys. Chem. B* **1997**, *101*, 7293.
(4) Reddy, N. R. S.; Wu, H.-M.; Jankowiak, R.; Picorel, R.; Codell, R. J.; Small, G. J. *Photosynth. Res.* **1996**, *48*, 277.
(5) Olsen, J. D.; Sockalingum, G. D.; Robert, B.; Hunter, C. N. *Proc. Natl. Acad. Sci. U.S.A.* **1994**, *91*, 7124.
(6) Fowler, G. J. S.; Sockalingum, G. D.; Robert, B.; Hunter, C. N. *Biochem. J.* **1994**, *299*, 697.
(7) Sturgis, J. N.; Olsen, J. D.; Robert, B.; Hunter, C. N. *Biochemistry* **1997**, *36*, 2772.
(8) Fowler, G. J. S.; Vischers, R. W.; Grief, G. G.; van Grondelle, R.; Hunter, C. N. *Nature (London)* **1992**, *355*, 848.
(9) Gall, A.; Fowler, G. J. S.; Hunter, C. N.; Robert, B. *Biochemistry* **1997**, *36*, 16282.
(10) Cogdell, R. J.; Isaacs, N. W.; Freer, A. A.; Arrelano, J.; Howard, T. D.; Papiz, M. Z.; Hawthornthwaite, A. M.; Prince, S. *Prog. Biophys. Mol. Biol.* **1997**, *68*, 1.
(11) Hanson, L. K. In *Chlorophylls*; Scheer, H., Ed.; CRC Press: Boca Raton, FL, 1991; pp 993−1014.
(12) Parson, W. W.; Warshel, A. *J. Am. Chem. Soc.* **1987**, *109*, 6152.
(13) Gudowsk-Nowak, E.; Newton, M. D.; Fajer, J. *J. Phys. Chem.* **1990**, *94*, 5795.
(14) Louwe, R. J. W.; Vrieze, J.; Hoff, A. J.; Aartsma, T. J. *J. Phys. Chem. B* **1997**, *101*, 11280.
(15) Fenna, R. E.; Matthews, B. W. *Nature (London)* **1975**, *258*, 573.
(16) Scholes, G. D.; Gould, I. R.; Cogdell, R. J.; Fleming, G. R. *J. Phys. Chem. B* **1999**, *103*, 2543.
(17) Hu, X.; Ritz, T.; Damjanovic, A.; Schulten, K. *J. Phys. Chem. B* **1997**, *101*, 3854.
(18) Linnanto, J.; Korppi-Tommola, J. E. I.; Helenius, V. M. *J. Phys. Chem. B* **1999**, *103*, 8739.
(19) Alden, R. G.; Nagarajan, V.; Parson, W. W.; Law, C. J.; Cogdell, R. G. *J. Phys. Chem. B* **1997**, *101*, 4667.
(20) Becke, A. D. *J. Chem. Phys.* **1993**, *98*, 5648.
(21) Frisch, M. J.; Trucks, G. W.; Schlegel, H. B.; Scuseria, G. E.; Robb, M. A.; Cheeseman, J. R.; Zakrzewski, V. G.; Montgomery, J. A., Jr.; Stratmann, R. E.; Burant, J. C.; Dapprich, S.; Millam, J. M.; Daniels, A. D.; Kudin, K. N.; Strain, M. C.; Farkas, O.; Tomasi, J.; Barone, V.; Cossi, M.; Cammi, R.; Mennucci, B.; Pomelli, C.; Adamo, C.; Clifford, S.; Ochterski, J.; Petersson, G. A.; Ayala, P. Y.; Cui, Q.; Morokuma, K.; Malick, D. K.; Rabuck, A. D.; Raghavachari, K.; Foresman, J. B.; Cioslowski, J.; Ortiz, J. V.; Stefanov, B. B.; Liu, G.; Liashenko, A.; Piskorz, P.; Komaromi, I.; Gomperts, R.; Martin, R. L.; Fox, D. J.; Keith, T.; Al-Laham, M. A.; Peng, C. Y.; Nanayakkara, A.; Gonzalez, C.; Challacombe, M.; Gill, P. M. W.; Johnson, B. G.; Chen, W.; Wong, M. W.; Andres, J. L.; Head-Gordon, M.; Replogle, E. S.; Pople, J. A. *Gaussian 98*; Gaussian, Inc.: Pittsburgh, PA, 1998.
(22) He, Z.; Sundström, V.; Pullerits, T. *Chem. Phys. Lett.* **2001**, *334*, 159.
(23) Crystal, J.; Friesner, R. A. *J. Phys. Chem. A* **2000**, *104*, 2362.
(24) Sundholm, D. *Chem. Phys. Lett.* **1999**, *302*, 480.
(25) Linnanto, J.; Korppi-Tommola, J. *J. Phys. Chem. A* **2001**, *105*, 3855.
(26) Petke, J. D.; Maggiora, G. M. *J. Chem. Phys.* **1986**, *84*, 1640.
(27) Crielaard, W.; Visschers, R. W.; Fowler, G. J. S.; van Grondelle, R.; Hellingwerf, J. J.; Hunter, C. N. *Biochim. Biophys. Acta* **1994**, *1183*, 473.
(28) Visschers, R. W.; Crielaard, W.; Fowler, G. J. S.; Hunter, C. N.; van Grondelle, R. *Biochim. Biophys. Acta* **1994**, *1183*, 483.
(29) Sturgis, J. N.; Jirsakova, V.; Reiss-Husson, F.; Cogdell, R. J.; Robert, B. *Biochemistry* **1995**, *34*, 517.
(30) Billeter, M.; Schaumann, T.; Braun, W.; Wüthrich, K. *Biopolymers* **1990**, *29*, 695.
(31) Fowler, G. J. S.; Hess, S.; Pullerits, T.; Sundström, V.; Hunter, C. N. *Biochemistry* **1997**, *36*, 11282.
(32) Gouterman, M. *J. Mol. Spectrosc.* **1961**, *6*, 138.
(33) Parusel, A. B. J.; Grimme, S. *J. Phys. Chem. B* **2000**, *104*, 5395.
(34) Hsu, C.-P.; Walla, P. J.; Head-Gordon, M.; Fleming, G. R. *J. Phys. Chem. B* **2001**, *105*, 11016.
(35) Herek, J. L.; Fraser, N. J.; Pullerits, T.; Martinsson, P.; Polivka, T.; Scheer, H.; Cogdell, R. J.; Sundström, V. *Biophys. J.* **2000**, *78*, 2590.
(36) Hartwich, G.; Fiedor, L.; Simonin, I.; Cmiel, E.; Schäfer, W.; Noy, D.; Scherz, A.; Scheer, H. *J. Am. Chem. Soc.* **1998**, *120*, 3675.
(37) Noy, D.; Yerushalmi, R.; Brumfeld, V.; Ashur, I.; Scheer, H.; Baldridge, K. K.; Scherz, A. *J. Am. Chem. Soc.* **2000**, *122*, 3937.